Pharmacogn. Res., 2025; 17(2):665-678.
https://www.phcogres.com

Original Article

Synergistic Effects of Guan-Xin-Er-Hao and Hydroxysafflor Yellow A on Atherosclerosis in ApoE$^{-/-}$ Mice: Unveiling Antioxidant and Anti-Inflammatory Mechanisms

Wenya Huang[1], Le Zhang[1], Li Zhou[1], Zhifang Cai[1], Kaige Wu[2], Yu Wang[2], Runze Zhou[1], Min Xu[1], Jia Li[1], Yunke Huang[1,3], Ping Ren[1], Xi Huang[1,*]

[1]Institute of Depression and Comorbidity, Nanjing University of Chinese Medicine, Nanjing, CHINA.
[2]Xiangya Hospital of Central South University, Changsha, CHINA.
[3]Women's Hospital School of Medicine, Zhejiang University, Hangzhou, CHINA.

ABSTRACT

Background: The Guan-Xin-Er-Hao (GXII) decoction, a traditional Chinese medicine, contains hydroxysafflor yellow A (HSYA) as its main active compound for treating coronary heart disease. **Objectives:** This study aimed to assess the therapeutic efficacy of HSYA compared to GXII and elucidate its molecular mechanisms in combating atherosclerosis. **Materials and Methods:** Guan-Xin-Er-Hao (GXII) was analyzed using HPLC-MS, which identified three main absorbable components: Hydroxysafflor Yellow A (HSYA), Ferulic Acid and Tanshinol. Among them, HSYA demonstrated the most pronounced effects in the *in vitro* experiments, leading to its selection for subsequent *in vivo* studies due to its high content and superior bioavailability within GXII. ApoE$^{-/-}$ mice were fed a high-fat diet for eight weeks and treated orally with GXII or HSYA. Atherosclerotic plaque areas and plasma lipid levels served as indicators of anti-atherosclerotic activity. Oxidative stress markers (malondialdehyde, superoxide dismutase, glutathione peroxidase, catalase) and inflammatory mediators (tumor necrosis factor-α, vascular cell adhesion molecule-1, interleukin-1β) were evaluated using enzyme-linked immunosorbent assays, western blotting and reverse transcription-polymerase chain reaction. **Results:** The Contribution Rate (CR) analysis indicated that HSYA significantly influenced serum lipid levels, oxidative stress markers and inflammatory protein/mRNA levels, with HSYA demonstrating a CR exceeding 90% relative to GXII. These findings underscore HSYA's predominant role within GXII in exerting anti-atherosclerotic effects through mitigation of oxidative stress and inflammation. **Conclusion:** The synergistic actions of GXII and HSYA reveal a promising therapeutic approach for atherosclerosis, offering valuable insights into their antioxidant and anti-inflammatory mechanisms in ApoE$^{-/-}$ mice.

Keywords: Anti-atherosclerosis, Anti-Inflammation, Antioxidant, Guan-Xin-Er-Hao, Hydroxysafflor yellow A.

Correspondence:
Prof. Xi Huang
Institute of Depression and Comorbidity, Nanjing University of Chinese Medicine, Nanjing-210023, CHINA.
Email: 290606@njucm.edu.cn

Received: 18-10-2024;
Revised: 07-01-2025;
Accepted: 04-03-2025.

INTRODUCTION

Atherosclerosis (AS) is a chronic inflammatory disease of the arterial wall caused by abnormal lipid metabolism.[1] It is the main pathological basis of acute coronary syndromes and major cardiovascular diseases, which cause high rates of mortality and morbidity worldwide.[2] Every year, more than 14 million individuals die of coronary AS and its complications.[3] Although many therapeutic techniques are available to treat patients with AS, the outcome remains unsatisfactory because of the inevitable side effects and high treatment expenditure. For example, simvastatin, a cholesterol synthesis inhibitor commonly used in the treatment of AS, causes numerous side effects, including joint pain, myopathy and memory impairment.[4] Therefore, describing the pathophysiology of AS is crucial to develop novel strategies for clinical treatment. Numerous studies have attempted to develop therapeutic strategies from Traditional Chinese Medicine (TCM). TCM is characterised by few side effects and has become an important source of natural products, such as hydroxysafflor yellow A, which exhibit significant protective effects on cardiovascular diseases.[5]

The process of AS development is accelerated by many factors, such as the release of inflammatory chemokines and cytokines, production of Reactive Oxygen Species (ROS) and growth factors and proliferation of vascular smooth muscle cells.[6-8] Oxidative stress reactions occur during the formation of

DOI: 10.5530/pres.20252095

atherosclerotic plaques,[9] whereas antioxidant molecules, such as Catalase (CAT), Superoxide Dismutase (SOD) and Glutathione Peroxidase (GSH-Px), can eliminate ROS and maintain cell redox homeostasis. When a large amount of ROS is produced in the endothelial cells, it causes lipid peroxidation and irreversible damage to cell membranes, proteins and DNA as well as oxidative damage to the blood vessel wall, which manifests as endothelial dysfunction. It is also accompanied by monocyte–macrophage migration, smooth muscle-cell formation, fibroblast proliferation and extracellular matrix degradation.

Tumour Necrosis Factor-α (TNF-α) is a proinflammatory cytokine produced by lipopolysaccharide-activated mononuclear phagocytes, which is highly expressed in patients with AS.[10] TNF-α damages myocardial mitochondrial electron transport complexes by increasing oxidative stress levels in cardiomyocytes.[11] TNF-α also triggers the expression of Vascular Cell Adhesion Molecule-1 (VCAM-1) in some immunological and inflammatory diseases.[12] During AS, VCAM-1 is mainly expressed in vascular endothelial cells where it participates in plaque formation by promoting the adhesion and migration of monocytes and endothelial cells.[13] Interleukin-1β (IL-1β), a proinflammatory cytokine, also plays an important role in the progression of arterial sclerosis.[14] Studies on coronary AS have revealed that blocking IL-1β reduces mortality rates.[15,16]

Guan-Xin-Er-Hao (GXII) decoction is a well-known TCM for coronary heart diseases. GXII increases coronary blood flow,[17] alleviates myocardial ischaemia,[18] reduces oxidative stress,[19] and inhibits inflammation[20] and anti-myocardial apoptosis.[21] Hydroxysafflor yellow A (HSYA), one of the components of GXII, is the main active pharmaceutical ingredient of safflower.[22] HSYA, also acts as an indicator of the medical value of safflower, as documented in the Pharmacopoeia of the People's Republic of China (2005 edition) and has been shown to be absorbed in rat or mouse blood.[23] Studies confirm that HSYA has broad pharmacological effects, such as antioxidant, anti-inflammatory and anticoagulant effects, which play vital roles in cardiovascular diseases.[24-26] However, the anti-atherosclerotic effect of HSYA has rarely been reported and the Contribution Rate (CR) of HSYA in GXII to ameliorate oxidative stress and inflammatory cytokine levels is unknown.

In this study, we aimed to describe the anti-atherosclerotic effects of GXII and its absorbed component HSYA based on the levels of oxidative stress indicators (Catalase [CAT]/Superoxide Dismutase [SOD]/Glutathione Peroxidase [GSH-Px]/Methane Dicarboxylic Aldehyde [MDA]) and inflammatory factors (VCAM-1/TNF-α/IL-1β) in High-Fat Diet (HFD)-fed ApoE$^{-/-}$ mice. The mechanisms through which GXII and HSYA ameliorate atherosclerosis are shown in Figure 1. Moreover, we compared the curative effect of HSYA and its parent herb GXII based on the CR of the monomers to the parent herb.[27] Thus, our research provides prospective insights into the anti-atherosclerotic effect of a TCM and its main ingredient.

MATERIALS AND METHODS

Preparation of GXII decoction and freeze-dried powder

All herbal materials (Table S1) were purchased from Xiangya Hospital of Central South University. GXII is a traditional Chinese herbal formula composed of salvia miltiorrhiza, ligusticum, chuanxiong, safflower, red peony and *Dalbergia odorifera* in a ratio of 2:1:1:1:1. The total mass of the crude drug was 90 g. We added 720 mL of purified water at a ratio of 1:8, soaked the drug for 30 min, boiled after decocting on a slow fire for 30 min, filtered with eight layers of gauze, added 720 mL of purified water, decocted according to the above method, filtered and combined the two filtrates to obtain the GXII decoction.

The GXII decoction was evaporated under reduced pressure in a rotary evaporator at 60°C to obtain a concentrated liquid, which was then uniformly condensed with liquid nitrogen and stuck to the wall of a glass freeze-dried bottle. The concentrated solution was freeze-dried in a vacuum freeze dryer at -55°C and <10 Pa for 24 hr to obtain a powder, which was sealed in a refrigerator at 4°C.

The content of three main active ingredients in GXII were determined using the UPLC-PDA method

The details of the three main active reference substances are provided in Table S1, with their molecular structures shown in Figure 1. The purity of all substances is greater than 98.0% and they have been identified as single chromatographic peaks by UPLC analysis.

Weighed precisely 3.2 mg of ferulic acid, 12.25 mg of hydroxy safflower yellow A, 6.36 mg of tanshinol sodium, 4.2 mg of protocatechuic aldehyde and 5.62 mg of paeoniflorin using a Sartorius SBP2llD analytical balance with a precision of 0.00001 g. These were placed into a 10 mL brown volumetric flask and 10 mL of methanol was added to bring the solution to the mark, followed by thorough ultrasonic dissolution to obtain the stock solutions of the five reference substances with concentrations of 320, 1225, 636, 420 and 562 ng/μL, respectively. Then, 0.5 mL of each stock solution was transferred into a 10 mL brown volumetric flask and 7.5 mL of methanol was added to bring the volume to the mark. The solutions were mixed thoroughly to obtain the mixed stock solution 1, with concentrations of ferulic acid 16 ng/μL, hydroxy safflower yellow A 61.25 ng/μL, tanshinol sodium 31.8 ng/μL, protocatechuic aldehyde 21 ng/μL and paeoniflorin 28.1 ng/μL. All reference solutions were sealed and stored in a 4°C refrigerator for future use.

To prepare the standard curve concentrations, the mixed stock solution 1 was diluted to generate five different concentrations

corresponding to 1/2, 1/4, 1/8, 1/16 and 1/32 of the original concentration, labeled as mixed stock solutions 2, 3, 4, 5 and 6, respectively. Then, 5 µL of each mixed stock solution (1 to 6), containing the standard substances for ferulic acid, hydroxy safflower yellow A, tanshinol sodium, protocatechuic aldehyde and paeoniflorin, was precisely aliquoted for injection. Under the chromatographic conditions described above, the peak areas (X) of each component's standard substance were measured and plotted against their corresponding concentrations (Y) to perform linear regression. This process allowed for the determination of the linear range and regression equation for each component. Additionally, the Limit of Detection (LOD) for each component was also determined (Table S2).

In vitro Experiment

RAW264.7 macrophages were selected as the target cells to establish an atherosclerotic foam cell model. The model was induced by treating macrophages with 100 µg/mL oxidized Low-Density Lipoprotein (ox-LDL). The experimental groups were as follows: Normal Group: Untreated macrophages. Model Group: Macrophages treated with ox-LDL (100 µg/mL). GPSDS Group: Cells treated with GXII-mediated serum after deproteinization. FA Group: Cells treated with ferulic acid (FA) at 162.82 ng/mL. HSYA Group: Cells treated with hydroxysafflor yellow A (HSYA) at 600 ng/mL. Tanshinol Group: Cells treated with tanshinol at 94.23 ng/mL. The levels of Triglycerides (TG), Tumor Necrosis Factor-alpha (TNF-α), Monocyte Chemoattractant Protein-1 (MCP-1) and intercellular adhesion molecule-1 (ICAM-1) in macrophages were quantified. Reactive Oxygen Species (ROS) production was analyzed using flow cytometry to measure mean fluorescence intensity and cell morphology was assessed using Oil Red O staining (refer to Supplementary Materials). Results demonstrated that all three primary components of GXII showed significant effects on the above indicators at plasma concentrations corresponding to their levels in ApoE$^{-/-}$ mice. Among them, HSYA exhibited the most pronounced effects, leading to its selection for subsequent *in vivo* studies due to its high content and superior bioavailability within GXII.

Cell Handling Procedure

All reagents were equilibrated to room temperature (18-25°C) for at least 30 min prior to use. Reagents were prepared according to the experimental protocol. Standard wells and test sample wells were set up and 100 µL of standard solution or test sample was added to each well. The plates were gently shaken to mix, covered with a plate seal and incubated at 37°C for 2 hr. After incubation, the liquid was discarded and the plates were spun dry without washing. Subsequently, 100 µL of biotin-labeled antibody working solution was added to each well and the plates were covered with a new seal and incubated at 37°C for 1 hr. After incubation, the liquid was discarded, the plates were spun dry and washed 3 times with 200 µL of wash buffer per well, soaking for 2 min each time. Next, 100 µL of horseradish peroxidase-labeled avidin working solution was added to each well and the plates were covered with a new seal and incubated at 37°C for 1 hr. The liquid was again discarded, the plates were spun dry and washed 5 times with 200 µL of wash buffer per well, soaking for 2 min each time. Finally, 90 µL of substrate solution was added to each well and color development was carried out at 37°C for 15-30 min in the dark. The reaction was stopped by adding 50 µL of stop solution to each well and the Optical Density (OD) at 450 nm was measured using a microplate reader within 5 min.

ROS Detection Procedure

The DCFH-DA stock solution (10 mM) was diluted 1:1000 in serum-free medium to achieve a final concentration of 10 µM. The cell culture medium was removed from the previously treated cells and an appropriate volume of the diluted DCFH-DA solution was added, ensuring the cells were fully covered. The cells were then incubated at 37°C for 20 min in a cell incubator. After incubation, the cells were washed three times with serum-free medium to remove any excess DCFH-DA. The cells were subsequently digested with trypsin, collected and analyzed for Reactive Oxygen Species (ROS) levels using flow cytometry.

Oil Red O Staining Procedure

The cells were rinsed with Phosphate-Buffered Saline (PBS) for 30 min, repeating the process six times and then incubated with Oil Red O staining solution at 37°C for 30 min. Following incubation, the cells were gently washed with distilled water and the stained cells were differentiated using 75% ethanol until the background appeared clear. The cells were then counterstained with hematoxylin for 5-10 min, rinsed with distilled water and returned to blue using PBS. Finally, the slides were mounted with buffered glycerol and observed under a microscope. This procedure ensured precise and reproducible results in evaluating the effects of GXII components, particularly HSYA, on foam cell formation and related biomarkers.

Preparation of HSYA

HSYA preparation safflower was purchased from Shanghai Yuanye Biotechnology Co., Ltd. The molecular weight of HSYA is 612.53 and its molecular structure is shown in Figure 1. The purity of HSYA used in this study was 98% (CAS NO.78281-02-A). HSYA was isolated from associate degree solution of false saffron extract mistreatment macroporous resin-gel activity, as antecedently delineate.[28] HSYA was dissolved in a traditional antiseptic saline for subsequent use.

Quantification of plasma HSYA levels using UPLC-MS/MS

Mice were orally administered with 11.7 g/kg GXII for eight weeks and blood samples were collected 30 min after the final

administration. After the plasma samples were treated, HSYA was detected via Ultra-Performance Liquid Chromatography-Mass Spectrometry (UPLC–MS) (Waters ACQUITY UPLC system H-Class, ACQUITY QDa mass detector) by comparing retention times and main products, providing a direct estimate of the anti-atherosclerotic effect of HSYA.

We used a Waters BEH (R) C18 analytical column (2.1 mm×100 mm, id 1.7μM) maintained at 30°C. The mobile phase consisted of methanol (A) and 0.1% formic acid (B) with the following gradient programme: 0-5 min, 90% B; 5-6 min, 40% B; 6-7 min, 10% B; 7-8 min, 90% B. The flow rate was set at 0.3 mL/min and the injection volume was 5 μL. The mass spectrum conditions were as follows: ion source, electrospray ion source, positive ion (ESI+); scanning mode, negative ion scanning detection methods, multi reaction monitoring; ion source temperature, 110°C; wavelength scanning, 200-600 nm for photodiode array detector; probe temperature, 600°C; capillary voltage, 0.8 kV; and acquisition type, full scan m/z 100-600, SIR scan m/z 261.08.

In vivo Experiment

40 SPF-grade 12-week-old male ApoE$^{-/-}$ mice (22±2 g) were provided by the Changzhou Carvens Laboratory Animal Co., Ltd, (Licence number: SCXK(苏)2021-0013). All animal care and experimental procedures were approved by the Animal Care and Use Committee of the Nanjing University of Chinese Medicine (Resolution No. 202204A016) and implemented in accordance with the National Institutes of Health Guidelines for the Nursing and Use of Laboratory Animals. After one week of adaptive feeding, the mice were administered their respective treatments by gavage (0.1 mL/10g) once a day for eight consecutive weeks to establish the AS model. Normal group: Normal Diet+Normal Saline (NS) by gavage; model group: high-fat diet (40% fat+1.25% cholesterol)+NS by gavage; simvastatin group: HFD+simvastatin suspension by gavage (10 mg/kg); GXII group: HFD+GXII decoction by gavage (11.7 g/kg); HSYA group: HFD+HSYA solution by gavage (1.95 mg/kg, dose equivalent to its content in GXII).

CR formula of monomers to parent herbs

$$\text{CR}\ (\%) = \frac{(2*Model-monomer)}{(2*Model-parent\ herbs)} \times 100\%$$

for indexes increasing after administration.

$$\text{CR}\ (\%) = \frac{monomer}{parent\ herbs} \times 100\%$$

for indexes decreasing after administration.

Biochemical determination of serum lipids

After eight weeks, the mice were fasted for 24 hr and blood samples were collected using a retro-orbital method. The samples were centrifuged at 3500 rpm for 10 min at 4°C and the upper serum was isolated. According to the manufacturer's instructions, the corresponding biochemical kits were used to determine Total Cholesterol (TC), Triglycerides (TG), Low-Density Lipoprotein Cholesterol (LDL-C) and High-Density Lipoprotein Cholesterol (HDL-C) levels.

Enzyme-linked immunosorbent assay to detect oxidative stress indicators

Blood samples were collected from the eyes of mice after being euthanised. The blood was centrifuged at 4°C and 12,000 rpm for 10 min and the serum isolated. Antioxidant activity of the serum was assessed according to MDA, SOD, CAT and GSH-Px levels. All procedures were performed using a diagnostic kit (Jiancheng, Nanjing, China) according to the manufacturer's instructions.

Haematoxylin and eosin staining assay of aortic arch paraffin sections

Haematoxylin and Eosin (HE) staining was performed according to conventional protocols.[29] After deparaffinisation and rehydration, 5 μM longitudinal sections were stained with haematoxylin solution for 5 min, dipped five times into 1% acid ethanol (1% HCl in 70% ethanol) and then rinsed in distilled water. The sections were then stained with eosin solution for 1-5 min, dehydrated with graded alcohol and cleared in xylene. The mounted slides were examined and photographed under a common light microscope (Leica, Germany).

Oil Red O staining assay of frozen aortic arch sections

After the mice were euthanised, the aortic arch was removed, placed in 4% paraformaldehyde overnight and cryosectioned. After drying, the sections were washed with 50% ethanol, stained with Oil Red O solution for 10 min, washed until the background was clear and counterstained with haematoxylin. Finally, the sections were sealed with glycerinated gelatin after drying, photographed and observed under an optical microscope (Leica). The ratio of aortic arch plaque area to lumen area was calculated using ImageJ software (US National Institutes of Health, Bethesda, MD, USA).

Western blot assay of inflammatory indicators

Protein concentrations in the thoracic abdominal aortas that were removed from the mice were determined using a BCA kit. The extracted protein was added to a loading buffer and boiled at 95°C for 5 min. After adding 50 μg of the sample to each well, the proteins were separated with 10% polyacrylamide gel electrophoresis and electrophoresed at 120 V and then transferred to polyvinylidene fluoride membranes with a wet transfer method at 100 V transmembrane voltage for 90 min. Thereafter, the membranes were blocked with 5% non-fat dry milk in Tris-Buffered Saline Tween-20 (TBST) for 1 hr at room temperature. Then, the membranes were incubated with anti-IL-1β, anti-TNF-α, anti-VCAM-1 (all diluted at 1:200), anti-β-actin (1:4000) and

anti-GAPDH (1:6000) primary antibodies overnight at 4°C. The membranes were washed three times with TBST for 5 min each and incubated for 1 hr at room temperature before adding the corresponding secondary antibody (1:2000 dilution, Abcam, Cambridge, MA, USA). After incubation, the membranes were washed three more times. Western blot signals were detected using Enhanced Chemiluminescence (ECL) and photographed using a Bio-Spectrum Gel Imaging System (UVP, USA).

Reverse Transcription-Polymerase Chain Reaction (RT-PCR) to detect inflammatory indicators

The mRNA coding sequences of TNF-α, VCAM-1, IL-1β and β-actin were determined using the National Center for Biotechnology Consensus Coding Sequences database. Details of the PCR primer sequences for TNF-α, VCAM-1, IL-1β and β-actin are summarised in Table S5. We homogenised mouse aortic tissue in liquid nitrogen and extracted RNA using the TRIzol reagent and an RNA extraction kit. The tissues were pyrolysed with 1 mL TRIzol for 5 min at room temperature, followed by centrifugation at 12000 rpm for 10 min. The supernatant was removed, mixed with 0.2 mL chloroform and centrifuged at 12000 rpm for 10 min. The aqueous phase was collected (~500 μL), supplemented with 250 μL absolute ethanol and run in the adsorption column for 45s. The adsorption column was washed with 500 μL of buffer and eluted with 80 μL H_2O. The RNA quality was determined using 1% agarose gel electrophoresis and RNA concentration by spectrophotometric detection.

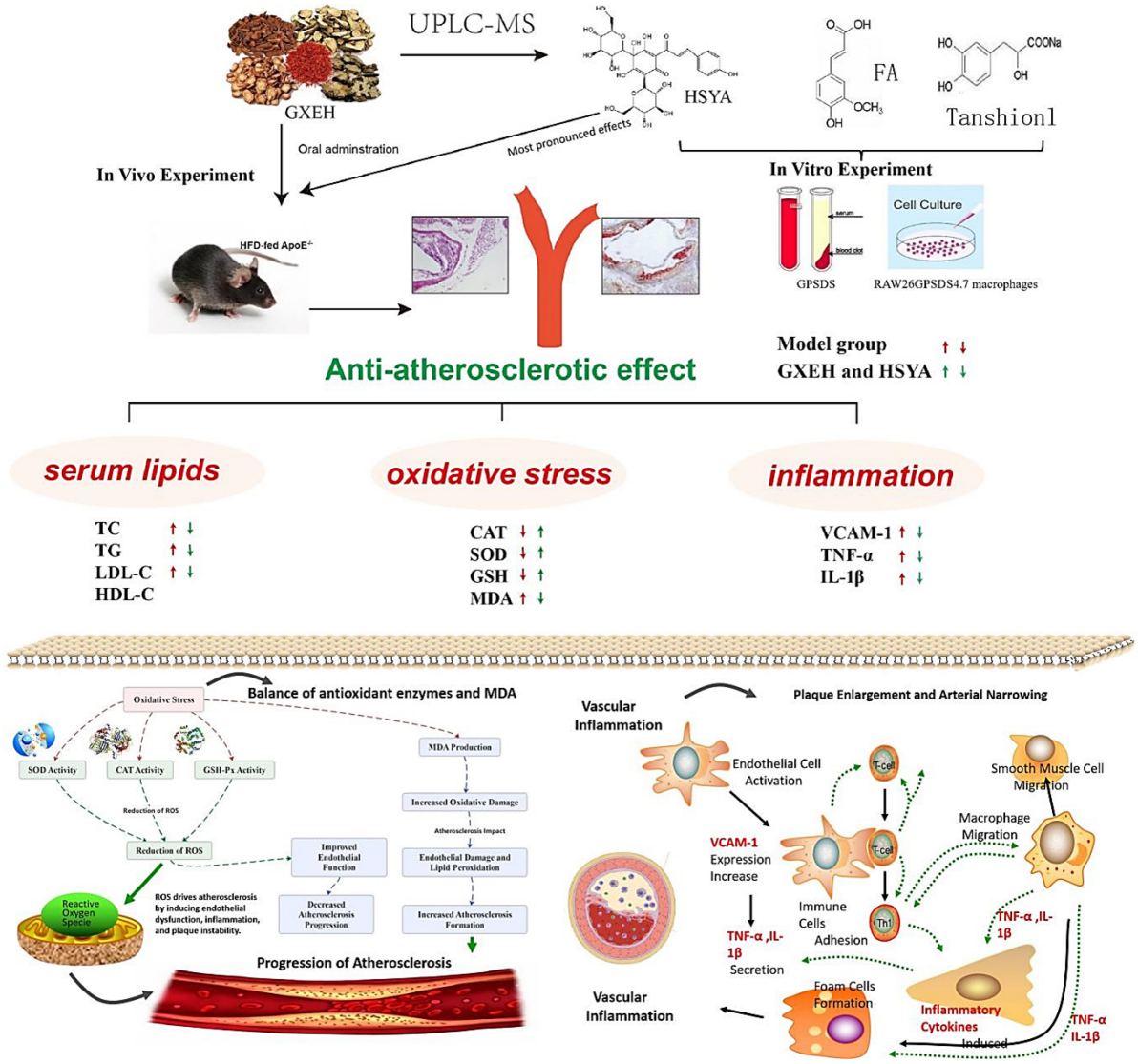

Figure 1: Mechanism of action of Guan-Xin-Er-Hao (GXII) and hydroxysafflor yellow A (HSYA) in ameliorating atherosclerosis in ApoE$^{-/-}$ mice involves antioxidant and anti-inflammatory effects. The figure illustrates the antioxidant and anti-inflammatory mechanisms of Guan-Xin-Er-Hao and Hydroxysafflor Yellow A. By balancing antioxidant enzymes and MDA production; they reduce Reactive Oxygen Species (ROS); thereby alleviating endothelial dysfunction and oxidative stress. ROS-induced inflammation increases VCAM-1 expression; promoting immune cell adhesion and migration; leading to foam cell formation and the secretion of inflammatory cytokines like TNF-α and IL-1β; which exacerbate atherosclerosis progression and vascular inflammation.

Statistical analysis

All data are expressed as mean±SD. A homogeneity of variance test was used for comparison between groups, one-way analysis of variance was used to analyse parametric data and the Kruskal-Wallis H test was used for non-parametric data. Differences between means were analysed using Fisher's protected LSD multiple comparison tests. All data were analysed using SPSS software version 16.0 (IBM SPSS, Chicago, IL, USA). Statistical significance was set at $p<0.05$.

RESULTS

Analysis of GXII decoction

The retention times and characteristic UV spectra of the five components in GXII decoction were identified within 15 min using the UPLC-PDA method, achieving good separation. The typical chromatograms of the main substances and GXII decoction are shown in Figure 2A. The three components Ferulic Acid (FA), hydroxysafflor yellow A and Tanshinol sodium were well separated in less than 25 min. Details of the main bioactive components in GXII decoction are presented in Supplementary Table S1.

Quantification of the three components in GXII decoction using UPLC-PDA

The quality control of GXII Decoction was performed using Ultra-Performance Liquid Chromatography (UPLC) to quantify its three main active components: Ferulic Acid (FA), Tanshinol (TAN) and Hydroxysafflor Yellow A (HSYA). The analysis revealed that the for TAN and 1949.61 ng/mL for HSYA (Table S2). These results provide a reliable quantitative basis for the quality assessment and standardization of GXII Decoction.

Quantification of the three components in Apoe$^{-/-}$ mice using UPLC-MS/MS

UPLC–MS/MS analysis of the serum samples in Apoe$^{-/-}$ mice showed no endogenous peak interference with the quantification of Ferulic acid, Tanshinol and Hydroxysafflor yellow A. Representative chromatograms of blank serum, blank serum spiked with FTA and internal standard (Acetaminophen 400 ng/mL) and extracted serum samples obtained 30 min after the oral administration of GXII (11.7 g/kg) decoction are shown in Figure 2B. As shown in Table S3, the standard calibration curves showed good determination coefficients (r>0.99) of all the analytes. The retention times of F, T, A and IS in serum were 5.56, 3.33, 4.69 and 3.60 min and the average concentration of FTA were 162.82 ng/mL, 94.23 ng/mL and 600.0 ng/mL, respectively.

Anti-atherosclerotic effect of of three main absorb components *in vitro* macrophage experiment

As shown in Figure 3A-D, compared with the normal group, the levels of TG, ICAM-1, TNF-α and MCP-1 in the model group were significantly increased with statistical significance ($^{\#\#}p<0.01$); The GPSDS group and the components groups (FA, HSYA, Tanshinol) decreased significantly ($^{**}p<0.01$). As shown in Figure 3E and Figure 3G, Levels of reactive oxygen species and the mean fluorescence intensity of ROS in the model group increased significantly comparing with the normal group ($\#\#p<0.01$); The GPSDS group and the components groups (FA, HSYA, Tanshinol) decreased significantly ($^{**}p<0.01$). As shown in Figure 3F and Figure 3H, after cell stained with Oil Red O, it was observed by light microscope that the staining effect of model group increased comparing with the normal group ($^{\#\#}p<0.01$); The GPSDS group and the components groups (FA, HSYA, Tanshinol) decreased significantly ($^{**}p<0.01$). *In vitro* cell experiments proved that the three main components in GXII had good effects on the above indicators in the blood drug absorption concentration of APOE$^{-/-}$ mice and HSYA had the most significant effect. Therefore, we selected HSYA for further *in vivo* studies because of its high content and high bioavailability in GXII.[18,22]

Effect of GXII and its absorbed component HSYA on serum lipid levels in ApoE$^{-/-}$ mice

We measured the effects of treatment with GXII and HSYA on serum lipid levels in HFD-fed ApoE$^{-/-}$ mice using an automatic biochemical analyser (Figure 4A-D). Compared with those of the normal group, the levels of TC, TG and LDL-C in HFD-fed ApoE$^{-/-}$ mice significantly increased ($p<0.01$), whereas no difference was observed in the level of HDL-C ($p>0.05$). Compared with those of the model group, the simvastatin group showed increased levels of TC and LDL-C ($p<0.01$) and decreased levels of TG ($p<0.01$) and both the GXII and HSYA groups showed decreased levels of TC, TG and LDL-C ($p<0.01$). No significant differences were observed in HDL-C levels between groups ($p>0.05$).

Treatment with HSYA and GXII lowered the levels of TC, TG, LDL-C and HDL-C ($p<0.01$). Compared with that of the model group, the CR of the HSYA group to the GXII group was >80% (TG: 10.79±0.24 vs 7.57±1.12 mmol/L; TC: 2.98±0.35 vs 2.51±0.23 mmol/L; LDL-C: 4.93±0.28 vs 4.49±0.23 mmol/L; Supplementary Table S4).

GXII and HSYA alleviated the morphological changes in the aortic arch in HFD-fed ApoE$^{-/-}$ mice

Morphological alterations in mouse aortic arches were observed using HE staining (Figure 4E). In the normal group, no plaque formation was observed, the intima was thin and smooth, no fractures were observed, the elastic plates inside and outside the vascular wall were clear and complete and the endothelium and smooth muscle cells were arranged evenly and neatly. In the model group, many flaky plaques, round or oval vacuolar foam cells, lipid deposition and inflammatory cell aggregation were observed. The three-layer structure of the blood vessel wall was disordered and unclear, with severe atrophy of the media, proliferation of smooth muscle cells and hyperplasia

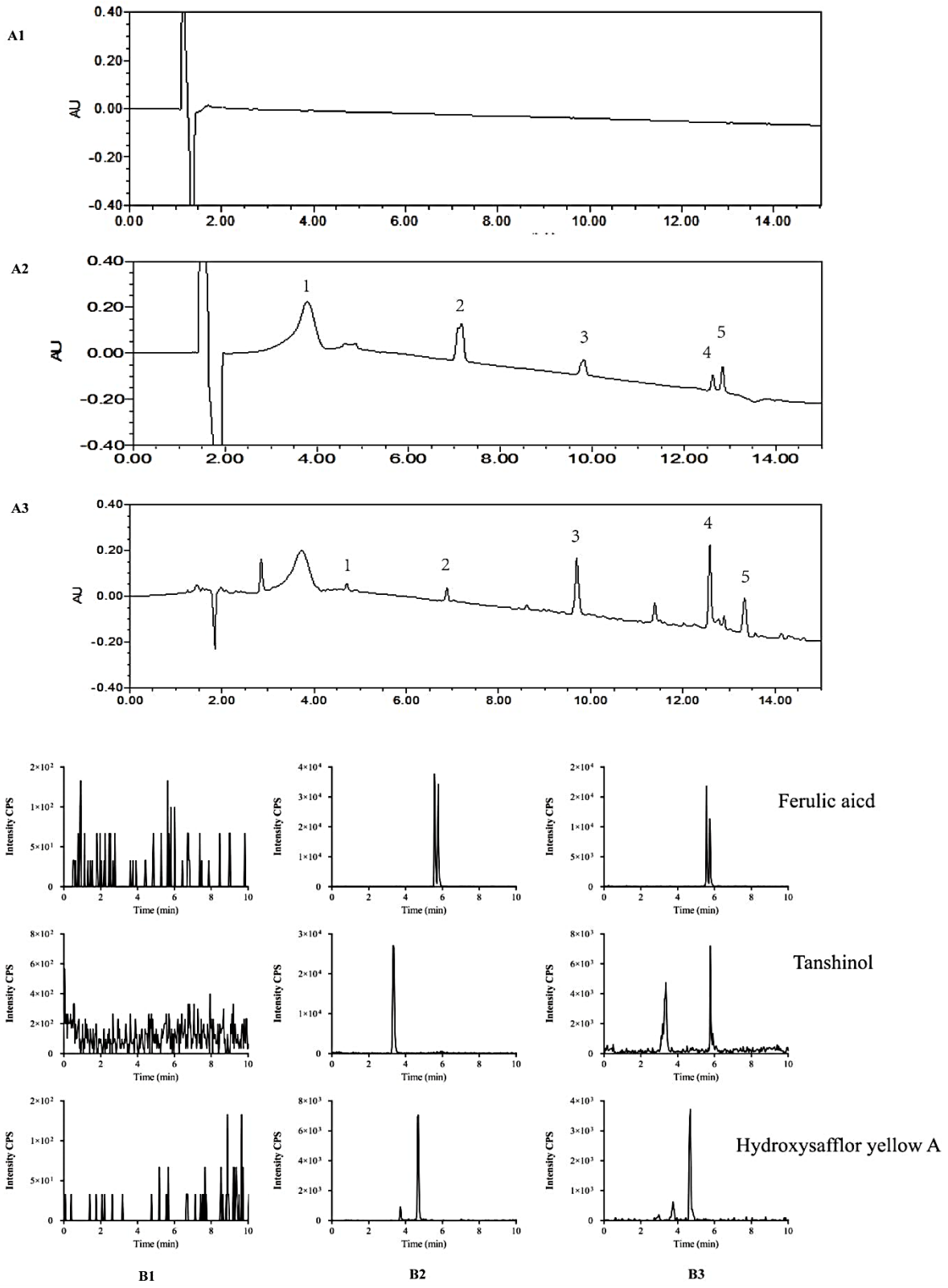

Figure 2: Ultra-Performance Liquid Chromatography (UPLC) Analysis of Guan-Xin-Er-Hao (GXII) and Quantification of Key Absorbable Components in ApoE$^{-/-}$ Mice Serum. A: Ultra-performance liquid chromatography of Guan-Xin-Er-Hao. A1: Blank solution; A2: Blank solution spiked with five control article (1. tanshinol; 2. protocatechualdehyde; 3. hydroxysafflor yellow A; 4. peoniflorin; 5. ferulaic acid); A3: Sample collected from GXEH (1. tanshinol; 2. protocatechualdehyde; 3. hydroxysafflor yellow A; 4. peoniflorin; 5. ferulaic acid). B: Chromatograms for the quantification of three main absorb components in Apoe-/- mice serum samples. Chromatograms of (B1) Blank serum; (B2) blank serum spiked with FTA and internal standard (Acetaminophen 400 ng/mL); and (B3) serum samples 30min after oral administration of GXII (11.7g/kg) to Apoe-/- mice.

(obvious irregular thickening, atheroma formation and a large number of vesicle cells and lipid cores). Beneath the fibre caps of atherosclerotic plaques, the arrangement of smooth muscle fibres was evidently disordered and many foam cells, cholesterol crystals and inflammatory cells were observed. Compared with those of the model group, fewer plaques were observed in the aortic arches of the GXII and HSYA groups and the infiltration of foam cells and inflammatory cells under the atherosclerotic plaques was reduced. The three-layer structure of the blood vessel wall was still clear and the arrangement of endothelial and smooth muscle cells was neat with some crisscrossing.

GXII and HSYA alleviated atherosclerotic plaque formation in HFD-fed ApoE$^{-/-}$ mice

We investigated the effect of GXII and HSYA on AS with a cross-sectional analysis of the atherosclerotic plaque areas using Oil Red O staining. As shown in Figure 4G, the lumen wall of the aortic arch in the normal group was smooth without plaque formation, whereas varying degrees of atherosclerotic plaque formation were observed in HFD-fed ApoE$^{-/-}$ mice. Treatment with GXII and HSYA significantly alleviated atherosclerotic lesions compared with those in the model group.

Oil Red O staining of aortic arch AS lesions showed that the plaque area in the model group accounted for 43.25±3.70% of the entire vessel lumen area, 28.88±2.37% in the simvastatin group, 30.20±2.37% in the control group and 35.63±2.06% in the HSYA group (Figure 4F). Compared with that of the model group, the plaque area in the GXII and HSYA groups was reduced by 30.17% (p<0.01) and 17.62% (p<0.01), respectively. A statistically significant difference was observed in the plaque area between the GXII and HSYA groups (p<0.05).

Treatment with HSYA and GXII (p<0.01) ameliorated the formation of atherosclerotic plaques. Compared with that of the model group, the CR of the HSYA group to the GXII group was >90% (plaque:surface ratio: 35.63±2.06% vs 30.20±1.48%; Supplementary Table S4).

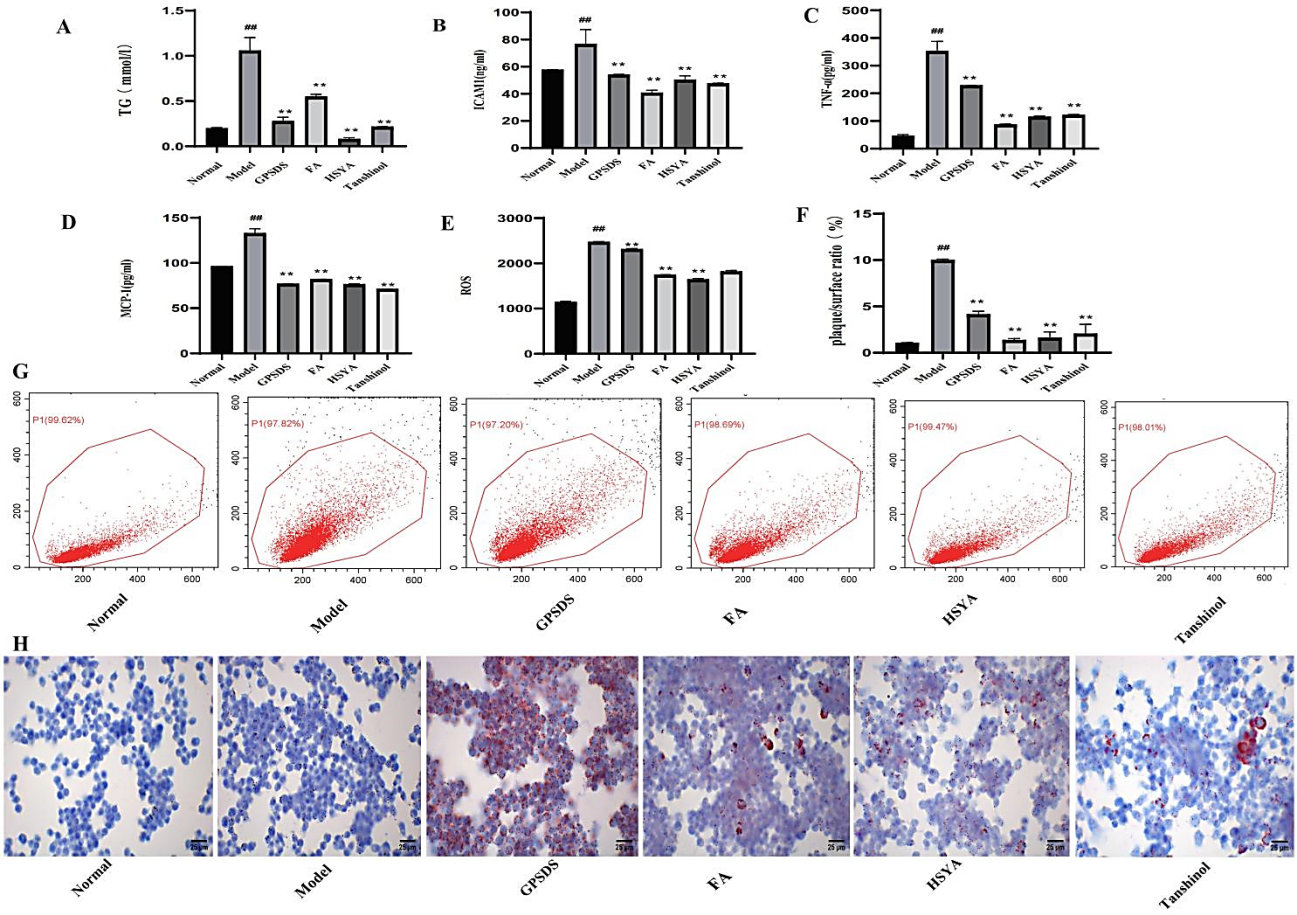

Figure 3: Anti-atherosclerotic effect of three main absorb components *in vitro* macrophage experiment. (A) Levels of Triglycerides (TG); (B) Levels of Intercellular Adhesion Molecule (ICAM)-1; (C) Levels of Tumour Necrosis Factor-α (TNF-α); (D) Levels of Monocyte Chemotactic Protein (MCP)-1; (E) Levels of Reactive Oxygen Species (ROS); (F) Ratio of oil red staining;(G) Mean fluorescence intensity of ROS; (H) Cell morphology of oil red staining. Data are presented as the mean±SD (n=3 for each group). #p<0.05; ##p<0.01; and ###p<0.001 versus the normal group. *p< 0.05; **p< 0.01; and ***p<0.001 versus the model group.

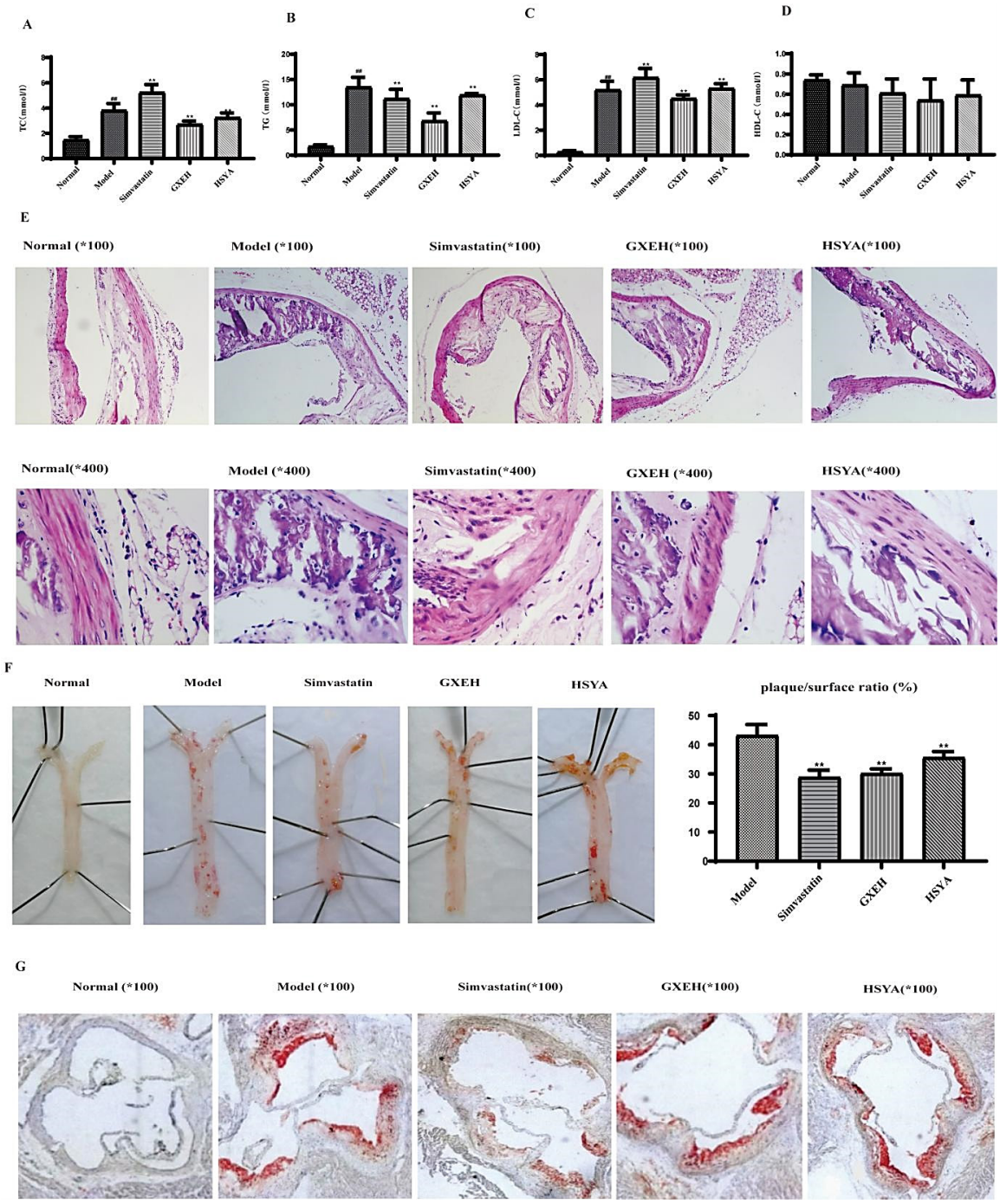

Figure 4: Effect of treatment with Guan-Xin-Er-Hao (GXII) and hydroxysafflor yellow A (HSYA) on serum lipid levels along with morphological changes of aortic arches and atherosclerotic plaque formation in ApoE$^{-/-}$ mice. Mice were treated with GXII (11.7 g/kg); HSYA (1.95 mg/kg); simvastatin (10 mg/kg); or normal saline for eight weeks. Serum lipids levels of Total Cholesterol (TC; A); Triglycerides (TG; B); Low-Density Lipoprotein Cholesterol (LDL-C; C); and High-Density Lipoprotein Cholesterol (HDL-C; D) were detected by biochemical analysis. E: The morphological changes of aortic arch [100×(upper row) and 400×(bottom row)] were evaluated by haematoxylin and eosin staining of paraffin sections. F: Representative aortic arch plaque image of whole aorta and quantification analysis of aortic arch plaque area accounts for the vascular lumen area. G: Cross section of aortic arch (100×) in frozen section stained with Oil Red O. Data are presented as the mean±SD (n=8 for each group). #p<0.05; ##p<0.01; and ###p<0.001 versus the normal group. *p<0.05; **p<0.01; and ***p<0.001 versus the model group.

Effects of treatment with GXII and HSYA on serum oxidative stress indicators in ApoE$^{-/-}$ mice

The serum MDA levels in the model, simvastatin, GXII and HSYA groups were significantly higher (p<0.05) and the levels of serum CAT, SOD and GSH-Px were significantly lower (p<0.05) than those of the normal group. Compared with those of the model group, the MDA levels of the simvastatin, GXII and HSYA groups significantly decreased (p<0.05) and the levels of serum CAT,

SOD and GSH-Px significantly increased (p<0.05). A statistically significant difference was observed in the levels of oxidative stress indicators between the GXII and HSYA groups (p<0.05, Figure 5A).

Notably, the CR of HSYA in determining the serum levels of MDA, SOD, GSH-Px and CAT was similar to that of GXII (MDA: 8.15±0.37 vs 6.05±0.49 nmol/mL; SOD: 126.00±4.13 vs 137.00±2.00 U/mL; GSH-Px: 0.53±0.06 vs 0.85±0.09 ng/mL; CAT: 627.55±44.44 vs 896.08±59.04 nmol/mL; Supplementary Table S4).

Effect of treatment with GXII and HSYA on the protein expression of inflammatory indicators in ApoE$^{-/-}$ mice analysed using western blotting

Compared with those of the normal group, TNF-α, VCAM-1 and IL-1β protein expression levels increased in the model, simvastatin, GXII and HSYA groups (p<0.01, Figure 5B). The expression levels of TNF-α, VCAM-1 and IL-1β in the simvastatin, GXII and HSYA groups significantly decreased (p<0.01) compared with those of the model group. A statistically significant difference was observed in the levels of inflammatory indicators between the GXII and HSYA groups (p<0.05).

Notably, similar CRs were observed for the thoracic aorta expression of TNF-α, VCAM-1 and IL-1β proteins induced by HSYA and GXII (TNF-α: 0.54±0.04 vs 0.45±0.02; VCAM-1: 0.52±0.02 vs 0.45±0.03; IL-1β: 0.51±0.03 vs 0.41±0.01; Supplementary Table S5).

Effect of treatment with GXII and HSYA on the mRNA levels of inflammatory indicators in ApoE$^{-/-}$ mice analysed using RT-PCR

Compared with those of the normal group, TNF-α, VCAM-1 and IL-1β mRNA expression levels increased in the model, simvastatin, GXII and HSYA groups (p<0.05, Figure 5C). The expression levels of TNF-α, VCAM-1 and IL-1β mRNAs were significantly lower in the simvastatin, GXII and HSYA groups (p<0.01) than those in the model group. The differences in the levels of inflammatory indicators were statistically significant between the GXII and HSYA groups (p<0.05).

Similar CRs were observed for the changes in mRNA levels of TNF-α, VCAM-1 and IL-1β induced by HSYA and GXII (TNF-α: 3.85±0.29 vs 2.50±0.20; VCAM-1: 3.58±0.17 vs 2.65±0.46; IL-1β: 3.99±0.26 vs 2.61±0.23; Supplementary Table S5).

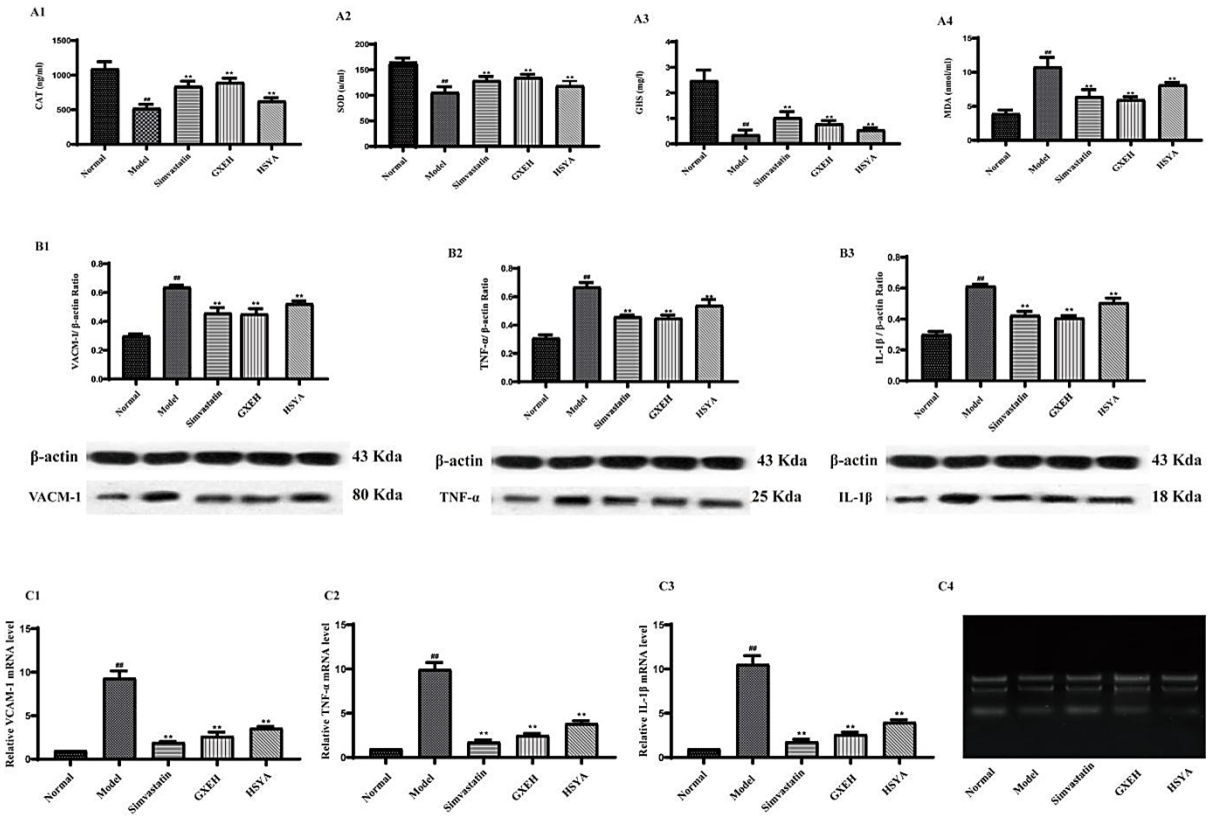

Figure 5: Effect of Guan-Xin-Er-Hao (GXII) and hydroxysafflor yellow A (HSYA) treatment on serum oxidative stress indicators and inflammatory indicators in ApoE$^{-/-}$ mice. Mice were treated with GXII (11.7 g/kg); HSYA (1.95 mg/kg); simvastatin (10 mg/kg); or Normal Saline (NS) for eight weeks. (A1) Catalase (CAT); (A2) Superoxide dismutase (SOD); (A3) Glutathione (GSH); (A4) Malondialdehyde (MDA) levels. (B1) Vascular cell adhesion molecule-1 (VCAM-1); (B2) Tumour necrosis factor-α (TNF-α); (B3) Interleukin-1β (IL-1β). (C1) Vascular cell adhesion molecule-1 (VCAM-1); (C2) Tumour Necrosis Factor-α (TNF-α); (C3) Interleukin-1β (IL-1β); (C4) Electrophoretic map of RNA: three bands with 28S; 18S; and 5S RNA from top to bottom. Data are presented as the mean±SD (n=8 for each group). #p<0.05; ##p<0.01; and ###p<0.001 versus the normal group. *p<0.05; **p<0.01; and ***p<0.001 versus the model group.

DISCUSSION

Hyperlipidaemia is a major risk factor of AS. According to an epidemiological study, increased levels of blood lipids are closely associated with the development and progression of AS.[30] In humans, TC and TG levels were significantly elevated in most cases of AS and were positively associated with disease severity.[31] LDL-C contributed to the pathogenesis of AS and low levels of LDL-C were associated with atheroprotection.[32] Previous studies have revealed that TG/TC/LDL-C are major contributors to cardiovascular diseases.[33] Evidently, HFDs cause increased levels of blood lipids, including TC, TG and LDL-C, which may cause hyperlipidaemia and aggravate AS.[34] In this study, ApoE$^{-/-}$ mice were fed an HFD for eight weeks to establish a coronary AS model. Our serum lipid results are consistent with the literature and the increasing levels of TC, TG and LDL-C in HFD-fed ApoE$^{-/-}$ mice and the appearance in atherosclerotic lesions in their aortic arches suggested that the AS model was successfully established. Morphological changes in the aortic arch detected by HE staining revealed foam cells, lipid deposits and inflammatory cell aggregation in model aortic plaques. Oil Red O staining of aortic arch AS lesions showed that the plaque area in the model group accounted for 43.25±3.70% of the entire vessel lumen area. Notably, our results demonstrated that GXII and its absorbed component HSYA were effective in reducing serum lipid TG/TC/LDL-C levels in atherosclerotic ApoE$^{-/-}$ mice. The atherosclerotic changes in the aortic arches were reversed by treatment with GXII and HSYA. HDL-C reportedly plays a crucial role in AS protection and elevated HDL-C levels negatively correlate with AS.[35] However, our results found no significant differences in HDL-C levels among the study groups, suggesting that the level of atherosclerotic changes in this study may not be severe enough to cause a significant change in HDL-C levels.

Oxidative stress plays an important role in the development of AS.[36] Normally, oxidation and anti-oxidation activities occur in a dynamic balance and antioxidant enzymes remove ROS and maintain cell redox homeostasis. However, under conditions of high ROS production and low antioxidant enzyme activity, peroxidative damage occurs in DNA, RNA, proteins and lipids, causing cell dysfunction and promoting the development of AS-related diseases.[37] CAT is a scavenger enzyme that breaks down hydrogen peroxide to oxygen and water, thus protecting cells from hydrogen peroxide poisoning and is one of the key enzymes in the biological defence system.[38] SOD is an antioxidant enzyme widely present in organisms that can catalyse superoxide free radicals to generate hydrogen peroxide and molecular oxygen and prevents organisms from the damage caused by oxygen free radicals generated in the metabolic process.[39] Another important antioxidant enzyme GSH-Px functions to eliminate hydrogen peroxide.[40] CAT reduces the proliferation of vascular smooth muscle cells[13]; SOD prevents the formation of peroxynitrite and reduces the levels of F2-isoprostaglandin and isofuran in the aorta.[41] GSH-Px inhibits the expression of monocyte chemoattractant protein-1 and VCAM-1.[42] These antioxidant enzymes collaborate to protect blood vessels against AS.[43] MDA is a sensitive indicator of lipid peroxidation and its level indirectly reflects the degree of oxygen radical damage.[44] Studies have shown that the balance between free radical production and *in vivo* clearance is disrupted during hyperlipidaemia, with enhanced lipid peroxidation, increased MDA levels and decreased SOD activity, leading to endothelial cell damage and AS.[45] The results of our present study are consistent with those of previous studies-the serum MDA levels in the AS model groups increased. This supports the effect of oxygen radical damage in AS and the decreasing levels of serum CAT, SOD and GSH-Px in the model groups, which is due to the protective effect of antioxidants in the vascular wall. Furthermore, HSYA and GXII effectively reduced the serum levels of MDA and elevated the serum levels of CAT, SOD and GSH-Px. Therefore, our findings support the anti-atherosclerotic effect of HSYA and GXII in ameliorating oxidative stress injury and maintaining the balance of endogenous antioxidant levels. Thus, lipid peroxidation was attenuated and AS was alleviated in HFD-fed ApoE$^{-/-}$ mice treated with HSYA and GXII.

Adhesion of monocytes and lymphocytes to the endothelium of the vascular wall plays an important role in AS. Atherosclerotic adhesion is achieved by various adhesion molecules located on the cell surface, including Intercellular Adhesion Molecule-1 (ICAM-1) and VCAM-1. Recent studies have revealed that the molecular mechanism of resveratrol inhibited the transcription of cell adhesion molecules and stimulated anti-atherogenic effect. VCAM-1 is a membrane protein that mediates the binding of monocytes to endothelial cells in the early stages of AS.[46] Inflammatory cytokines, such as TNF-α and IL-1β, stimulates VCAM-1 expression in vascular endothelial cells and cause inflammatory conditions in monocytes,[47] which implies that overexpression of VCAM-1 contributes to vascular inflammation. Here, we demonstrated that both the protein and mRNA levels of VCAM-1 in HFD-fed ApoE$^{-/-}$mice significantly increased, which indicated an increased atherosclerotic adhesion effect. This suggests that HSYA and GXII attenuated AS in mice by decreasing VCAM-1 levels. TNF-α is an early inflammatory biomarker for AS that can predict cardiovascular events and is involved in the initial stages of AS.[48] Genetic and pharmacological inhibition experiments have shown that focal adhesion kinase regulates VCAM-1 expression by preventing TNF-α-induced VCAM-1 expression within heart vessel-associated endothelial cells *in vivo*.[49] IL-1β is expressed in atherosclerotic plaques that are composed of epithelial tissue cells and macrophages in the coronary arteries of patients with anaemia.[50] A lack of IL-1β reduces the severity of AS in ApoE$^{-/-}$ mice by regulating VCAM-1 expression in arterial blood vessels.[51] Similarly, our study demonstrated increased levels of TNF-α, IL-1β and VCAM-1 in the AS model group. Treatment with HSYA and GXII reduced

the levels of these proinflammatory factors (VCAM-1/TNF-α/IL-1β), suggesting that the anti-AS effects of the intervention might be ascribed to the anti-inflammatory effects of the HSYA and GXII. Guan-Xin-Er-Hao (GXEH) and Hydroxysafflor Yellow A (HSYA) exhibit significant antioxidant and anti-inflammatory effects, which play a crucial role in mitigating atherosclerosis. By balancing antioxidant enzymes and reducing Malondialdehyde (MDA) production, these compounds decrease oxidative stress and endothelial dysfunction. They enhance antioxidant enzyme activity (SOD, CAT, GSH-Px), reducing Reactive Oxygen Species (ROS) that cause inflammation and plaque instability. ROS increase VCAM-1 expression, promoting immune cell adhesion and foam cell formation, which in turn triggers the release of inflammatory cytokines like TNF-α and IL-1β. These mechanisms help alleviate vascular inflammation and atherosclerosis progression (Figure 1).

The concept of 'biological prescription analysis of traditional Chinese medicine' was first proposed by our research group, where we characterised the pharmacological aspects of prescriptions into Bioethnopharmaceutical Analytical Pharmacology (BAP).[18] The BAP strategy consists of two parts: (1) quality control of prescriptions and (2) comparative study of the efficacy of absorbable components and their parent formulas. Both parts were incorporated in the present study. For quality control of a prescription, a method that can determine the Absorbed Bioactive Compound (ABC) levels in the body is required. We used UPLC to determine the levels of the three main active ingredients (FA/TAN/hydroxysafflor yellow A) in GXII decoction with the following results: FA, 128.84 ng/mL; TAN, 270.38 ng/mL; and HSYA, 1949.61 ng/mL. We further used UPLC-MS to determine the plasma concentrations of the three components in mice administered with 11.7 g/kg GXII (FA, 20.4 ng/mL; TAN, 6.9 ng/mL; and HSYA, 154.0 ng/mL). In our previous study, we showed that the effective substances of the compound can be easily revealed by controlling the administered dose.[52] Our previous studies adopted the strategy of using an *in vitro* administration dose that was equal to the content of the bioactive compound and showed that the cardioprotective function of GXII was associated with the absorbed bioactive components.[18] Thus, we used an *in vitro* dose of HSYA equal to the content in GXII to verify whether HSYA exerted the anti-atherosclerotic effect of GXII as an absorbed bioactive component. For the second part of BAP, we compared the curative effect of HSYA and its parent herb GXII according to the CR of monomers to the parent herb.

According to the relative CR, HSYA contributed a large fraction of the efficacy observed in the mother formula. The CR of HSYA to reductions in serum TG, TC and LDL-C levels and decreases in plaque area in atherosclerotic ApoE$^{-/-}$ mice was 83.56%, 90.90%, 93.14% and 90.36%, respectively. Moreover, HSYA played an essential role in reducing the level of oxidative stress, contributing 86.56%, 91.97% and 70.03% to the efficacy of the mother formula in reducing the levels of oxidative stress indexes MDA, SOD and CAT, respectively. Furthermore, HSYA significantly improved the inflammatory response in mice. HSYA contributed substantially to the efficacy of its parent formula in altering the protein and mRNA levels of TNF-α (92.25%, 89.99%), VCAM-1 (94.18%, 91.39%) and IL-1β (92.53%, 87.96%), respectively. On comparing the curative effect of HSYA and its parent herb GXII, the present study confirms that HSYA is one of the main bioactive components of GXII.

CONCLUSION

In this study, ApoE$^{-/-}$ mice developed typical atherosclerotic lesions after being fed an HFD for eight weeks. After intragastric administration of GXII and HSYA, blood lipid levels and progression of atherosclerotic plaques in mice with AS lesions were successfully ameliorated. In addition, the intervention treatments induced anti-atherosclerotic effects by ameliorating serum lipid levels, suppressing oxidative stress indicators and regulating proinflammatory factors. Moreover, HSYA, the absorbed component of GXII, was found to be effectively absorbed in the blood of atherosclerotic ApoE$^{-/-}$ mice. We found that HSYA exerted effects similar to those of GXII, including anti-atherosclerotic, antioxidant and anti-inflammatory activities; it also decreased serum lipid levels. The highest CRs of HSYA to the curative effect of GXII reached >90%. Thus, the anti-atherosclerotic effect of GXII is from one of its main bioactive components HSYA. We have provided a basis for the anti-atherosclerotic effect of a TCM and its main ingredients by preliminarily clarifying the associated molecular mechanisms. Our study provides new perspectives on natural AS treatment approaches and will hopefully stimulate the international recognition of TCMs in AS-related clinical applications.

ACKNOWLEDGEMENT

The authors would like to thank the Institute of TCM-Related Comorbid Depression of the Nanjing University of Chinese Medicine and the Xiangya Hospital of Central South University for their invaluable contribution to the study. The authors would also like to thank he participants for volunteering in the study.

CONFLICT OF INTEREST

The authors declare no conflict of interest.

FUNDING

This work was supported by the National Natural Science Foundation of China (Grant number 81173591), the Priority Academic Program Development of Jiangsu Higher Education Institutions (Integration of Chinese and Western Medicine) and the Foundation for High-level Talents from the Nanjing University of Chinese Medicine (XH).

ABBREVIATIONS

TCM: Traditional Chinese medicines; **GXII:** Guan-Xin-Er-Hao; **FA:** Ferulic acid; **TAN**; Tanshinol; **HSYA:** Hydroxysafflor yellow A; **AS:** Atherosclerosis; **HFD:** High-fat diet; **MDA;** Methane dicarboxylic aldehyde; **SOD:** Superoxide dismutase; **GSH-Px:** Glutathione peroxidase; **CAT:** Catalase; **TNF-α:** Tumour necrosis factor-α; **VCAM-1:** Vascular cell adhesion molecule-1; **IL-1β:** Interleukin-1β; **CR:** Contribution rate; **TC:** Total cholesterol; **TG:** Triglycerides; **LDL-C:** Low-density lipoprotein cholesterol; **HDL-C:** High-density lipoprotein cholesterol; **UPLC-MS:** Ultra-performance liquid chromatography-mass spectrometry; **ELISA:** Enzyme-linked immunosorbent assays; **HE:** Haematoxylin and eosin; **RT-PCR:** Reverse transcription-polymerase chain reaction; **ICAM-1:** Intercellular adhesion molecule-1; **BAP:** Bioethnopharmaceutical analytical pharmacology; **ABC:** Absorbed Bioactive Compound.

ETHICAL STATEMENTS

All animal care and experimental procedures were approved by the Animal Care and Use Committee of the Nanjing University of Chinese Medicine (Resolution No. 202204A016) and implemented in accordance with the National Institutes of Health Guidelines for the Nursing and Use of Laboratory Animals.

SUMMARY

We investigated the therapeutic effects and molecular mechanisms of Hydroxysafflor yellow A (HSYA); the main active compound in the Traditional Chinese Medicine Guan-Xin-Er-Hao (GXII) decoction; in the treatment of atherosclerosis. Using an ApoE$^{-/-}$ mouse model fed a high-fat diet; we compared the efficacy of HSYA and GXII in reducing atherosclerotic plaque formation and plasma lipid levels. Key biomarkers of oxidative stress (malondialdehyde; superoxide dismutase; glutathione peroxidase; catalase) and inflammation (Tumor Necrosis Factor-α; vascular cell adhesion molecule-1; interleukin-1β) were analyzed through enzyme-linked immunosorbent assays; western blotting; and reverse transcription-polymerase chain reaction.

The Contribution Rate (CR) analysis revealed that HSYA accounted for over 90% of GXII's effects on lipid metabolism; oxidative stress reduction; and inflammation suppression. These results suggest that HSYA plays a dominant role in the anti-atherosclerotic activity of GXII by mitigating oxidative stress and inflammatory responses. This study highlights HSYA as a potential key therapeutic component for atherosclerosis treatment and provides insights into the pharmacological mechanisms of GXII decoction. Future research should explore the clinical applicability of HSYA and its potential for targeted therapy.

Guan-Xin-Er-Hao (GXII) was analyzed using HPLC-MS; which identified three main absorbable components: Hydroxysafflor Yellow A (HSYA); Ferulic Acid; and Tanshinol. Among them; HSYA demonstrated the most pronounced effects in the *in vitro* experiments; leading to its selection for subsequent *in vivo* studies due to its high content and superior bioavailability within GXII.

High-Fat Diet (HFD)-fed ApoE$^{-/-}$ mice; used as an atherosclerosis model; showed atherosclerotic changes; such as increased levels of Total Cholesterol (TC); Triglycerides (TG); and Low-Density Lipoprotein Cholesterol (LDL-C) and plaque area of the aortic arch; decreased serum levels of Catalase (CAT); Superoxide Dismutase (SOD); and Glutathione Peroxidase (GSH-Px); and increased levels of Methane Dicarboxylic Aldehyde (MDA) and the proinflammatory factors VCAM-1; TNF-α; and IL-1β. GXII and its absorbed component HSYA induced anti-atherosclerotic effects by ameliorating serum lipid levels; improving oxidative stress indicators; and regulating proinflammatory factors.

REFERENCES

1. Malekmohammad K, Bezsonov EE, Rafieian-Kopaei M. Role of lipid accumulation and inflammation in atherosclerosis: focus on molecular and cellular mechanisms. Front Cardiovasc Med. 2021;8:707529. doi: 10.3389/fcvm.2021.707529, PMID 34552965.
2. Wang Y, Cao F. *In vivo* MR and fluorescence dual-modality imaging of atherosclerosis characteristics in mice using Profilin-1 targeted magnetic nanoparticles. J Am Coll Cardiol. 2016;68S:C49.
3. Heestermans M, Ouweneel AB, Hassan J, Kloosterman M, Reitsma PH, Gijbels MJ, *et al.* Predilection of Low protein C-induced Spontaneous atherothrombosis for the Right Coronary Sinus in apolipoprotein E deficient mice. Sci Rep. 2018;8(1):15106. doi: 10.1038/s41598-018-32584-y, PMID 30305662.
4. Magni P, Macchi C, Morlotti B, Sirtori CR, Ruscica M. Risk identification and possible countermeasures for muscle adverse effects during statin therapy. Eur J Intern Med. 2015;26(2):82-8. doi: 10.1016/j.ejim.2015.01.002, PMID 25640999.
5. Zhao F, Wang P, Jiao Y, Zhang X, Chen D, Xu H, *et al.* A systematical review on botanical resources; physicochemical properties; drug delivery system; pharmacokinetics; and pharmacological effects. Front Pharmacol. 2020;11. doi: 10.3389/fphar.2020.579332.
6. Marchio P, Guerra-Ojeda S, Vila JM, Aldasoro M, Victor VM, Mauricio MD. Targeting early atherosclerosis: A focus on oxidative stress and inflammation. Oxid Med Cell Longev. 2019; 2019:8563845. doi: 10.1155/2019/8563845, PMID 31354915.
7. Wang K, Shang T, Zhang L, Zhou L, Liu C, Fu Y, *et al.* Application of a reactive oxygen species-responsive drug-eluting coating for surface modification of vascular stents. ACS Appl Mater Interfaces. 2021;13(30):35431-43. doi: 10.1021/acsami.1c08880, PMID 34304556.
8. Jiang L, Luo S, Qiu T, Li Q, Jiang C, Sun X, *et al.* Bidirectional role of reactive oxygen species during inflammasome activation in acrolein-induced human EAhy926 cells pyroptosis. Toxicol Mech Methods. 2021;31(9):680-9. doi: 10.1080/15376516.2021.1953204, PMID 34238121.
9. Bułdak Ł, Łabuzek K, Bułdak RJ, Machnik G, Bołdys A, Basiak M, *et al.* RETRACTION: metformin reduces the expression of NADPH oxidase and increases the expression of antioxidative enzymes in human monocytes/macrophages cultured *in vitro* (Retraction of Vol 11; Pg 1095; 2016). Exp Ther Med. 2017;13(2):794. doi: 10.3892/etm.2016.3973, PMID 28352368.
10. Al Shahi H, Shimada K, Miyauchi K, Yoshihara T, Sai E, Shiozawa T, *et al.* Elevated circulating levels of inflammatory markers in patients with acute coronary syndrome. Int J Vasc Med. 2015; 2015:805375. doi: 10.1155/2015/805375, PMID 26504600.
11. Li X, Guo D, Zhou H, Hu Y, Fang X, Chen Y, *et al.* Side Effects of Coronary stenting such as Severe Coronary stenosis and Multiple Coronary Chronic Total Occlusions in Elderly Patients via Induced proinflammatory and prooxidative Stress. Mediat Inflam. 2019; 2019:7147652. doi: 10.1155/2019/7147652, PMID 31780868.
12. Kong DH, Kim YK, Kim MR, Jang JH, Lee S. Emerging roles of vascular cell adhesion Molecule-1 (VCAM-1) in immunological disorders and cancer. Int J Mol Sci. 2018;19(4):1057. doi: 10.3390/ijms19041057, PMID 29614819.
13. Malekmohammad K, Sewell RD, Rafieian-Kopaei M. Antioxidants and atherosclerosis: mechanistic aspects. Biomolecules. 2019;9(8):301. doi: 10.3390/biom9080301, PMID 31349600.
14. Berg M, Polyzos KA, Agardh H, Baumgartner R, Forteza MJ, Kareinen I, *et al.* 3-Hydroxyanthralinic acid metabolism controls the hepatic SREBP/lipoprotein axis; inhibits inflammasome activation in macrophages; and decreases atherosclerosis in Ldlr(-/-) mice. Cardiovasc Res. 2020;116(12):1948-57. doi: 10.1093/cvr/cvz258, PMID 31589306.
15. Ridker PM, Everett BM, Thuren T, MacFadyen JG, Chang WH, Ballantyne C, *et al.* Antiinflammatory therapy with canakinumab for atherosclerotic disease. N Engl J Med. 2017;377(12):1119-31. doi: 10.1056/NEJMoa1707914, PMID 28845751.

16. Ridker PM, MacFadyen JG, Everett BM, Libby P, Thuren T, Glynn RJ, *et al.* Relationship of C-reactive protein reduction to cardiovascular event reduction following treatment with canakinumab: a secondary analysis from the CANTOS randomised controlled trial. Lancet. 2018;391(10118):319-28. doi: 10.1016/S0140-6736(17)32814-3, PMID 29146124.
17. Zeng X, He H, Yang J, Yang X, Wu L, Yu J, *et al.* Temporal effect of Guanxin No. 2 on cardiac function; blood viscosity and angiogenesis in rats after long-term occlusion of the left anterior descending coronary artery. J Ethnopharmacol. 2008;118(3):485-94. doi: 10.1016/j.jep.2008.05.017, PMID 18579111.
18. Huang X, Qin F, Zhang HM, Xiao HB, Wang LX, Zhang XY, *et al.* Cardioprotection by Guanxin II in rats with acute myocardial infarction is related to its three compounds. J Ethnopharmacol. 2009;121(2):268-73. doi: 10.1016/j.jep.2008.10.029, PMID 19041701.
19. Qin F, Liu YX, Zhao HW, Huang X, Ren P, Zhu ZY. Chinese medicinal formula Guan-Xin-Er-Hao protects the heart against oxidative stress induced by acute ischemic myocardial injury in rats. Phytomedicine. 2009;16(2-3):215-21. doi: 10.1016/j.phymed.2008.08.005, PMID 18951001.
20. Zhang XY, Huang X, Qin F, Ren P. Anti-inflammatory effect of Guan-Xin-Er-Hao via the nuclear factor-kappa B signaling pathway in rats with acute myocardial infarction. Exp Anim. 2010;59(2):207-14. doi: 10.1538/expanim.59.207, PMID 20484854.
21. Zhao HW, Qin F, Liu YX, Huang X, Ren P. Antiapoptotic mechanisms of Chinese medicine formula; Guan-Xin-Er-Hao; in the rat ischemic heart. Tohoku J Exp Med. 2008;216(4):309-16. doi: 10.1620/tjem.216.309, PMID 19060445.
22. Xue X, Deng Y, Wang J, Zhou M, Liao L, Wang C, *et al.* Hydroxysafflor yellow A; a natural compound from *Carthamus tinctorius* L with good effect of alleviating atherosclerosis. Phytomedicine. 2021;91:153694. doi: 10.1016/j.phymed.2021.153694, PMID 34403879.
23. Wang Y, Huang X, Qin F, Ren P, Zhu Z, Fan R, *et al.* A strategy for detecting optimal ratio of cardioprotection-dependent three compounds as quality control of Guan-Xin-Er-Hao formula. J Ethnopharmacol. 2011;133(2):735-42. doi: 10.1016/j.jep.2010.11.006, PMID 21073938.
24. Bacchetti T, Morresi C, Bellachioma L, Ferretti G. Antioxidant and pro-oxidant properties of *Carthamus tinctorius*; hydroxy safflor yellow A; and safflor yellow A. Antioxidants (Basel). 2020;9(2):119. doi: 10.3390/antiox9020119, PMID 32013224.
25. Luo M, Huang JC, Yang ZQ, Wang YS, Guo B, Yue ZP. Hydroxysafflor yellow A exerts beneficial effects by restoring hormone secretion and alleviating oxidative stress in polycystic ovary syndrome mice. Exp Physiol. 2020;105(2):282-92. doi: 10.1113/EP088147, PMID 31803965.
26. Qin X, Chen J, Zhang G, Li C, Zhu J, Xue H, *et al.* Hydroxysafflor yellow A exerts anti-inflammatory effects mediated by SIRT1 in lipopolysaccharide-induced microglia activation. Front Pharmacol. 2020;11:1315. doi: 10.3389/fphar.2020.01315, PMID 33041785.
27. Huang Y, Xu M, Li J, Chen K, Xia L, Wang W, et al. *Ex vivo* to *in vivo* extrapolation of syringic acid and ferulic acid as grape juice proxies for endothelium-dependent vasodilation: redefining vasoprotective resveratrol of the French paradox. Food Chem. 2021;363:130323. doi: 10.1016/j.foodchem.2021.130323, PMID 34247035.
28. Zheng M, Guo X, Pan R, Gao J, Zang B, Jin M. Hydroxysafflor yellow A alleviates ovalbumin-induced asthma in a guinea pig model by attenuateing the expression of inflammatory cytokines and signal transduction. Front Pharmacol. 2019;10:328. doi: 10.3389/fphar.2019.00328, PMID 31024302.
29. Guo Y, Wang L, Ma R, Mu Q, Yu N, Zhang Y, *et al.* JiangTang XiaoKe granule attenuates cathepsin K expression and improves IGF-1 expression in the bone of high fat diet induced KK-Ay diabetic mice. Life Sci. 2016;148:24-30. doi: 10.1016/j.lfs.2016.02.056, PMID 26892148.
30. Tsukinoki R, Okamura T, Watanabe M, Kokubo Y, Higashiyama A, Nishimura K, *et al.* Blood pressure; low-density lipoprotein cholesterol; and incidences of coronary artery disease and ischemic stroke in Japanese: the Suita study. Am J Hypertens. 2014;27(11):1362-9. doi: 10.1093/ajh/hpu059, PMID 24713850.
31. Chapman MJ, Ginsberg HN, Amarenco P, Andreotti F, Borén J, Catapano AL, *et al.* Triglyceride-rich lipoproteins and high-density lipoprotein cholesterol in patients at high risk of cardiovascular disease: evidence and guidance for management. Eur Heart J. 2011;32(11):1345-61. doi: 10.1093/eurheartj/ehr112, PMID 21531743.
32. Shapiro MD, Fazio S. Apolipoprotein B-containing lipoproteins and atherosclerotic cardiovascular disease. F1000Res. 2017;6:134. doi: 10.12688/f1000research.9845.1, PMID 28299190.
33. Kathiresan S, Manning AK, Demissie S, D'Agostino RB, Surti A, Guiducci C, *et al.* A genome-wide association study for blood lipid phenotypes in the Framingham Heart Study. BMC Med Genet. 2007; 8 Suppl 1:S17. doi: 10.1186/1471-2350-8-S1-S17, PMID 17903299.
34. Kobayashi Y, Inagawa H, Kohchi C, Kazumura K, Tsuchiya H, Miwa T, *et al.* Oral administration of *Pantoea agglomerans*-derived lipopolysaccharide prevents development of atherosclerosis in high-fat diet-fed apoE-deficient mice via ameliorating hyperlipidemia; pro-inflammatory mediators and oxidative responses. PLOS One. 2018;13(3):e0195008. doi: 10.1371/journal.pone.0195008, PMID 29584779.
35. Li L, Yu AL, Wang ZL, Chen K, Zheng W, Zhou JJ, *et al.* Chaihu-Shugan-San and absorbed meranzin hydrate induce anti-atherosclerosis and behavioral improvements in high-fat diet ApoE−/− mice via anti-inflammatory and BDNF-TrkB pathway. Biomed Pharmacother. 2019;115:108893. doi: 10.1016/j.biopha.2019.108893, PMID 31022598.
36. Yang X, Li Y, Li Y, Ren X, Zhang X, Hu D, *et al.* Oxidative stress-mediated atherosclerosis: mechanisms and therapies. Front Physiol. 2017;8:600. doi: 10.3389/fphys.2017.00600 , PMID 28878685.
37. Ohsawa I, Ishikawa M, Takahashi K, Watanabe M, Nishimaki K, Yamagata K, *et al.* Hydrogen acts as a therapeutic antioxidant by selectively reducing cytotoxic oxygen radicals. Nat Med. 2007;13(6):688-94. doi: 10.1038/nm1577, PMID 17486089.
38. Chelikani P, Fita I, Loewen PC. Diversity of structures and properties among catalases. Cell Mol Life Sci. 2004;61(2):192-208. doi: 10.1007/s00018-003-3206-5, PMID 14745498.
39. Bannister JV, Bannister WH, Rotilio G. Aspects of the structure; function; and applications of superoxide dismutase. CRC Crit Rev Biochem. 1987;22(2):111-80. doi: 10.3109/10409238709083738, PMID 3315461.
40. Nadkarni GD, Sawant BU. Role of antioxidant defence in renal pathophysiology: primacy of glutathione peroxidase. Indian J Exp Biol. 1998;36(6):615-7. PMID 9731475.
41. Yang H, Zhou L, Wang Z; Roberts LJI; Lin X; Zhao Y; Guo Z. Overexpression of antioxidant enzymes in ApoE-deficient mice suppresses Benzo(a) pyrene-accelerated atherosclerosis. Atherosclerosis. 2009;207:51-58. DOI: 10.1016/j.atherosclerosis.2009.03.052.
42. Wagner AH, Kautz O, Fricke K, Zerr-Fouineau M, Demicheva E, Gueldenzoph B, *et al.* Upregulation of glutathione peroxidase offsets stretch-induced proatherogenic gene expression in human endothelial cells. Arterioscl Throm Vasc. 2009;29:1454-894. doi: 10.1161/ATVBAHA.109.194738.
43. Lönn ME, Dennis JM, Stocker R. Actions of "antioxidants" in the protection against atherosclerosis. Free Radic Biol Med. 2012;53(4):863-84. doi: 10.1016/j.freeradbiomed.2012.05.027, PMID 22664312.
44. Xia W, Liu G, Shao Z, Xu E, Yuan H, Liu J, *et al.* Toxicology of tramadol following chronic exposure based on metabolomics of the cerebrum in mice. Sci Rep. 2020;10(1):11130. doi: 10.1038/s41598-020-67974-8, PMID 32636435.
45. Plump AS, Smith JD, Hayek T, Aalto-Setälä K, Walsh A, Verstuyft JG, *et al.* Severe hypercholesterolemia and atherosclerosis in apolipoprotein E-deficient mice created by homologous recombination in ES cells. Cell. 1992;71(2):343-53. doi: 10.1016/0092-8674(92)90362-G, PMID 1423598.
46. Lusis AJ. Atherosclerosis. Nature. 2000;407(6801):233-41. doi: 10.1038/35025203, PMID 11001066.
47. Lim ST, Miller NL, Chen XL, Tancioni I, Walsh CT, Lawson C, *et al.* Nuclear-localized focal adhesion kinase regulates inflammatory VCAM-1 expression. J Cell Biol. 2012;197(7):907-19. doi: 10.1083/jcb.201109067, PMID 22734001.
48. Tibaut M, Caprnda M, Kubatka P, Sinkovič A, Valentova V, Filipova S, *et al.* Markers of atherosclerosis: Part 1- Serological Markers. Heart Lung Circ. 2019;28(5):667-77. doi: 10.1016/j.hlc.2018.06.1057, PMID 30468147.
49. Lim ST, Miller NL, Chen XL, Tancioni I, Walsh CT, Lawson C, *et al.* Nuclear-localized focal adhesion kinase regulates inflammatory VCAM-1 expression. J Cell Biol. 2012;197(7):907-19. doi: 10.1083/jcb.201109067, PMID 22734001.
50. Galea J, Armstrong J, Gadsdon P, Holden H, Francis SE, Holt CM. Interleukin-1 beta in coronary arteries of patients with ischemic heart disease. Arterioscler Thromb Vasc Biol. 1996;16(8):1000-6. doi: 10.1161/01.ATV.16.8.1000, PMID 8696938.
51. Kirii H, Niwa T, Yamada Y, Wada H, Saito K, Iwakura Y, *et al.* Lack of interleukin-1beta decreases the severity of atherosclerosis in ApoE-deficient mice. Arterioscler Thromb Vasc Biol. 2003;23(4):656-60. doi: 10.1161/01.ATV.0000064374.15232.C3, PMID 12615675.
52. Shi S, Yan H, Chen Y, Liu Y, Zhang X, Xie Y, *et al.* Pharmacokinetic study of precisely representative antidepressant; prokinetic; anti-inflammatory and anti-oxidative compounds from *Fructus aurantii* and Magnolia Bark. Chem Biol Interact. 2020;315:108851. doi: 10.1016/j.cbi.2019.108851, PMID 31614129.

Cite this article: Huang W, Zhang L, Zhou L, Cai Z, Wu K, Wang Y, *et al*. Synergistic Effects of Guan-Xin-Er-Hao and Hydroxysafflor Yellow A on Atherosclerosis in ApoE-/- Mice: Unveiling Antioxidant and Anti-Inflammatory Mechanisms. Pharmacog Res. 2025;17(2):665-78.

Table S1: Main herbal materials in GXEH decoction.

Name of herbal	Latin name	Producing area	Voucher number
Salvia miltiorrhiza	*Salvia miltiorrhiza* Bunge	Shanxi	170901
Ligusticum chuanxiong	*Ligusticum chuanxiong* Hort	Sichuan	170501-1
Safflower	*Carthamus tinctorius* L	Xinjiang	170901
Red peony	*Radix paeoniae* Rubra	Nei Monggol	170902
Dalbergia odorifera	*Dalbergia odorifera* T. Chen	Hainan	170911

The details of the three main active ingredients in GXEH.

Bioactive components	Molecular formula	Formula weight	CAS number	Company	Lot number	Source herbal
Ferulic acid	$C_{10}H_{10}O_4$	194.19	1135-24-6	Shanghai Yuanyuan Biotechnology Co.; LTD	YY20110722	Ligusticum chuanxiong
Hydroxysafflor yellow A	$C_{27}H_{32}O_{16}$	612.53	78281-02-A	Shanghai Yuanyuan Biotechnology Co.; LTD	YY20100819	Safflower
Tanshinol sodium	$C_9H_9NaO_5$	200.16	67920-52-9	Shanghai Yuanyuan Biotechnology Co.; LTD	YY20110411	-

Table S2: The standard curve; linear range; and limit of detection for the three components were determined; and the results for these components in GXEH decoction were subsequently analyzed.

Bioactive components		Ferulic acid	Hydroxysafflor yellow A	Tanshinol sodium
Regression equation		Y=41304X-96494	Y=15666X-24690	Y=22970X-1.4E+5
Regression coefficient (R2)		0.9926	0.9932	0.9919
Linearity range (ng/uL)		0.50-16.00	1.91-61.25	0.99-31.80
Lowest detectable limit (μg /uL)		0.09	0.32	0.21
Content of active ingredients (ng/mg)	Powder1	129.20	1951.24	273.00
	Powder2	129.19	1947.27	267.46
	Powder3	128.13	1950.32	270.68
Average Content (ng/mg)		128.84±0.47	1949.61±1.56	270.38±1.95
RSD (%)		0.36%	0.08%	0.72%

Table S3: Standard curve; linear range; and concentration of FTA in serum.

Bioactive components	TR (min)	Calibration curves	Regression coefficient (R2)	Linear range (μg/mL)	concentration (ng/mL)
F	5.56	y=1.78e3x+2.74e3	0.9991	0.02-2	162.82
T	3.33	y=238x-864	0.9972	0.05-2	94.23
A	4.69	y=65x-135	0.9978	0.05-2	600.0

Table S4: Contribution rate of serum lipids levels and plaque/surface ratio; and serum oxidative stress indicators.

	TG (mmol/L)	TC (mmol/L)	HDL-C (mmol/L)	LDL-C (mmol/L)	Plaque/ surface ratio (%)	MDA (nmol/ mL)	SOD (U/mL)	GSH (ng/ mL)	CAT (nmol/mL)
Control	1.680±0.311	1.355±0.233	0.670±0.01	0.255±0.035		3.96± 0.12	164.0± 3.56	2.49±0.18	1089.72±103.92
Model	13.580±1.584	3.805±0.304	0.680± 0.071	5.445±0.445	43.25± 3.70	10.8± 0.97	112.0± 4.00	0.39±0.05	521.34±57.50
Simvastatin	11.080±1.289	5.130±0.448	0.560±0.082	7.010±0.348	28.88± 2.37	6.54± 0.86	133.0 ± 0.036	1.01±0.06	840.05±71.83
GXEH	7.570±1.122	2.513±0.231	0.440±0.171	4.493±0.226	30.20± 1.48	6.05± 0.49	137.0± 2.00	0.85±0.09	896.08±59.04
HSYA/X±SD	10.790±0.243	2.977±0.346	0.607±0.055	4.93±0.28	35.63± 2.06	8.15± 0.37	126.0± 4.13	0.53±0.06	627.55±44.44
Contribution/%	83.56%	90.90%		93.14%	90.36%	86.50%	91.97%	62.35%	70.03%

Table S5: Contribution rate of the protein and mRNA expression of the inflammatory indicators and PCR primer information.

	Western blot (β-actin)			RT-PCR		
	TNF-α	VCAM-1	IL-1β	TNF-α	VCAM-1	IL-1β
Control	0.314±0.022	0.301±0.013	0.301±0.018	1.00±0.00	1.00±0.00	1.00±0.00
Model	0.665±0.028	0.639±0.011	0.615±0.010	9.96±0.76	9.31±0.83	10.54±0.97
Simvastatin	0.464±0.013	0.460±0.036	0.426±0.024	1.75±0.22	1.94±0.10	1.80±0.25
GXEH	0.451±0.020	0.453±0.034	0.408±0.014	2.50±0.20	2.65±0.46	2.61±0.23
HSYA/X±SD	0.539±0.037	0.524±0.017	0.507±0.028	3.85±0.29	3.58±0.17	3.99±0.26
Contribution/%	89.99%	91.39%	87.96%	92.25%	94.18%	92.53%

PCR primer information.

mRNA Primers	Sequence (5′–3′)	Product length (bp)
Mice-β-IL-1β-F	CGTTCCCATTAGACAACTGCA	206
Mice-β-IL-1β-R	GGTATAGATTCTTTCCTTTGAGGC	228
Mice-β-TNF-α-F	TGAGGACCAAGGAGGAAAGTATG	99
Mice-β-TNF-α-R	T CAGCAGGTGTCGTTGTTCAGG	116
Mice-β-VCAM-1-F	TGGAAATGTGCCGAAAC	
Mice-β-VCAM-1-R	GCCTGGCGGATGGTGTA	
Mice-β-actin-F	CATCCTGCGTCTGGACCTGG	
Mice-β-actin-R	TAATGTCACGCACGATTTCC	